



Article

Synergistic Effects of Functional CNTs and h-BN on Enhanced Thermal Conductivity of Epoxy/Cyanate Matrix Composites

Mingzhen Xu *, Yangxue Lei, Dengxun Ren, Sijing Chen, Lin Chen and Xiaobo Liu *

Research Branch of Advanced Functional Materials, School of Materials and Energy, University of Electronic Science and Technology of China, Chengdu 610054, China; leiyangxue@163.com (Y.L.); rendenxun2008@126.com (D.R.); csj20189@126.com (S.C.); chenlin_uestc@163.com (L.C.)

* Correspondence: mzxu628@uestc.edu.cn (M.X.); liuxb@uestc.edu.cn (X.L.); Tel.: +86-028-8320-7326 (X.L.); Fax: +86-028-8320-7326 (X.L.)

Received: 6 November 2018; Accepted: 29 November 2018; Published: 3 December 2018



Abstract: Epoxy/cyanate resin matrix composites (AG80/CE) with improved thermal conductivity and mechanical properties were obtained with synergetic enhancement with functional carbon nanotubes (*f*-CNTs) and hexagonal boron nitride (h-BN). AG80/CE performed as polymeric matrix and h-BN as conductivity filler which formed the main thermal conductivity channels. Small amounts of *f*-CNTs were introduced to repair defects in conductivity channels and networks. To confirm the synergetic enhancements, the thermal conductivity was investigated and analyzed with Agari's model. Results indicated that with introduction of 0.5 wt% *f*-CNTs, the thermal conductivity coefficient (λ) increased to 0.745 W/mk, which is 1.38 times that of composites with just h-BN. Furthermore, the flexural strength and modulus of composites with 0.5 wt% *f*-CNTs were 85 MPa and 3.5 GPa. The glass transition temperature (T_g) of composites with 0.4 wt% was 285 °C and the initial decomposition temperature ($T_{5\%}$) was 385 °C, indicating outstanding thermal stability. The obtained h-BN/*f*-CNTs reinforced AG80/CE composites present great potential for packaging continuous integration and miniaturization of microelectronic devices.

Keywords: nanoparticles; copolymerization; functional CNTs; h-BN; cyanate ester

1. Introduction

The miniaturization and multi-functionality integration of electronic components have increased rapidly, and have demanded higher requirements on polymeric substrates because the rapidly increasing thermal accumulation of inner polymeric substrates can influence the performance and working reliability of substrate materials [1–4]. Thus, the designing and fabrication of polymeric composites with high thermal conductivities, satisfactory mechanical properties, and ideal thermal stabilities have become necessary. Moreover, it is also imperative to realize heat transfer by the substrate materials themselves, to prolong service life and avoid functional damage to components [5,6].

Epoxy resin and cyanate ester have been widely applied in the fields of electronics, automobile, sensor, aerospace, machinery, and chemical engineering, due to their excellent mechanical strength, friction resistance and electrical insulation, superior chemical resistance, good thermal and dimensional stability, and easy processing [7–11]. However, the relatively low thermal conductive coefficient (λ) of pristine epoxy resin and the cyanate ester matrix has limited their wider application [3,12].

As is well known, it is too difficult to fabricate a resin matrix with an intrinsic higher λ value than (>0.50 W/mK). Thus, thermally conductive inorganic fillers have been incorporated into polymeric composites to improve their thermal conductivity. As reported previously, addition of single thermally conductive fillers, including SiO₂ [13], Al₂O₃ [14], BN [5,6,8], AlN [15], SiC [16],

Si₃N₄ [17], CNTs [18], graphite nano-platelets [3,19], graphene oxide [1], graphene [11], etc. in epoxy resin matrices was investigated and results indicated that their thermal conductivities can be enhanced. Moreover, hybrid thermally conductive fillers, including Al₂O₃/AlN [20], AlN/BN, AlN/multi-wall carbon nanotubes (MWCNTs) [21], Cu/MWCNTs [22], SiO₂/graphene oxide [23], BN/graphene oxide [24], graphite nanoplatelets/SiC [25], graphite nanoplatelets/CNTs [26], nanosilica/AgNWs, etc. were also introduced, and improved thermal conductivities of epoxy composites were obtained. Previous researches have achieved reasonable results. However, the researches were focused on category, shape, size, volume, and mass fraction, as well as surface functionalization of single and/or hybrid thermally conductive fillers on the thermal conductivities of epoxy composites, which limited their generalization in other high-performance resin matrices [2,9,11]. Furthermore, relatively high loading of thermally conductive fillers introduced into the resin matrix also results in adverse impacts on the processing behaviors and mechanical properties of the designed composites.

It is well known that the thermal conductivity of resin matrix composites with conductive fillers has been dominated by thermal conductivity channels and networks formed with fillers in the matrices [2,27]. Thus, the ability of fillers to form conductivity channels and networks as well as contact and overlap of fillers determined by the content of fillers, directly affects the thermal conductivity of the resulting composites [2,3,5,6,10]. In our previous work, epoxy/cyanate resin composites with various contents of h-BN were prepared and the results indicated that on increasing the content of h-BN, the thermal conductivity of the composites increased [28]. According to Agari's model, with h-BN in the matrix it is hard to form effective conductivity channels [9]. Moreover, on continuous increase in the content of h-BN, the process behaviors of epoxy resin matrices worsen and it is difficult to obtain model composites. Additionally, the mechanical properties of the composites decrease significantly, which limits applications in the field of structural components. The decreases of mechanical properties has been mentioned in many reports [2,5,29].

In this work, it is proposed that in the case of a certain content of fillers in the resin matrix, improving the ability of fillers to form conductivity channels and networks can be expected to result in composites with satisfactory mechanical properties and improved thermal conductivity. Herein, functional CNTs (*f*-CNTs) and h-BN were introduced into the epoxy/cyanate resin matrix to obtain composites with improved combination properties. The effects of *f*-CNT content on thermal conductivity, mechanical properties, and thermal stability were investigated. Also, the synergetic enhancements of *f*-CNTs and h-BN on combination properties are also discussed.

2. Materials and Methods

2.1. Materials

CNTs (diameters: 10–30 nm, purity: >95%) were supplied by Chengdu Organic Chemistry Co. Ltd., Chinese Academy of Sciences, Chengdu, China. Carboxyl functionalized CNTs (*f*-CNTs) were prepared as previously reported [30]: raw CNTs were sonicated in a mixture of concentrated sulfuric and nitric acid (3:1 by volume) for 1 h at 60 °C. The solid was centrifuged and dried in a vacuum. The bisphenol A-based cyanate ester resin, 4,4'-(propane-2,2-diyl)bis(cyanatobenzene), was supplied by Wuqiao Resins Co. Ltd. (Yangzhou, China). Epoxy resin, AG80 (Equal Molar Weight (EMW) = 117–134 g/mol) was obtained from Shanghai Huaxi Resins Co. Ltd. (Shanghai, China). Hexagonal boron nitride (h-BN) powders were purchased from Macklin and used as received without further purification. Imidazole was used as initiator. Moreover, the thermal conductivity coefficients of the starting materials used in this work are presented in Table 1.

Table 1. Thermal conductivity coefficients of starting materials.

Samples	Thermal Conductivity Coefficients (λ , W/mk)
Neat matrix resin	0.26 [28]
Hexagonal boron nitride (h-BN)	300
Carbon nanotube (CNT)	6600
Composites with 0.5 wt% <i>f</i> -CNT	0.32 (experiment data)

2.2. Preparation of the h-BN/*f*-CNTs Reinforced Matrix Blends

The required amount of epoxy resin and cyanate with a weight ratio of 4:6 was mixed and melted at 100 °C, with 0.5 wt% imidazole added as the latent initiator. Then, 40 wt% (weight of h-BN to the matrix) content of h-BN was added, with stirring for another 1 h. Various amounts of functional CNTs (*f*-CNTs) were added into the viscous solution with rapid stirring for another 2 h. The *f*-CNTs proportions were as follows: 0 wt%, 0.3 wt%, 0.4 wt%, and 0.5 wt% (weight of CNTs to the matrix), respectively. Then, the h-BN/*f*-CNT reinforced matrix blends were poured into molds and rapidly cooled to room temperature. The various blends were labeled as h-BN/*f*-CNTs/Matrix-0, h-BN/*f*-CNTs/Matrix-0.3, h-BN/*f*-CNTs/Matrix-0.4, h-BN/*f*-CNTs/Matrix-0.5, respectively, according to the various contents of *f*-CNTs.

2.3. Preparation of the h-BN/*f*-CNTs Reinforced Matrix Composites

First, a polytetrafluoroethylene mold with cavity dimensions 50 mm × 10 mm × 3 mm was preheated at 120 °C for 2 h. Then, the h-BN/*f*-CNTs/Matrix blending was melted at 100 °C for 20 min and the viscous melt was poured into the preheated polytetrafluoroethylene mold to carry out the standard procedure. The cured h-BN/*f*-CNT/Matrix composites were sanded to a thickness of 2 mm for dynamic mechanical measurements (DMA). Also, the cured h-BN/*f*-CNTs/Matrix composites were physically pulverized at ambient conditions for thermal gravimetric analysis (TGA).

2.4. Characterizations

Scanning electron microscope (SEM, JSM25900LV) was employed to observe the morphology of the functional CNTs and the fractured surfaces of the composites. X-ray photoelectron spectroscopic (XPS) measurements were carried out on an ESCA 2000 (VG Microtech, Uckfield, UK) using a monochromic Al K α ($h\nu = 1486.6$ eV) X-ray source. Differential scanning calorimetric analysis (DSC) with a nitrogen flow rate of 50 mL/min and a heating rate of 10 °C/min was used to investigate the curing behavior of the blends. TGA was performed on a TA Instruments TGA Q50 with a heating rate of 20 °C/min (under nitrogen or air) and a purge flow rate of 40 mL/min. Thermal conductivity was measured with a Netzsch LFA 457 Laser Flash Apparatus. Mechanical properties were tested by flexural experiments with the three-point bending mode using the SANS CMT6104 series desktop electromechanical universal testing machine (CMT6104, Shenzhen, China) and a moving speed of crosshead displacement of 5 mm/min. Samples with dimension 50 mm × 10 mm × 1.2 mm were tested with the ratio of support span to thickness of 15:1. Results were obtained from the average value of three samples. Dynamic mechanical analysis (DMA) in a three-point-bending mode was performed on a QDMA-800 dynamic mechanical analyzer (TA Instruments, New Castle, DE, USA) to determine the glass temperature (T_g). The storage modulus, tan delta, and glass transition temperature (T_g) were studied with an amplitude of 15 μ m and a frequency of 1 Hz, while the composites were all heated from 50 °C to 350 °C with a temperature ramp of 3 °C/min.

3. Results

3.1. Morphology and Structures of *f*-CNTs

Functional CNTs (*f*-CNTs) were prepared by acidizing and characterized mainly by SEM and XPS, shown in Figures 1 and 2. In Figure 1a, the pristine CNTs are presented in large length-diameter ratios,

which resulted in serious aggregation. It can be observed in Figure 1a that the aggregation is mainly ascribed to entanglement of the long CNTs. In comparison to that of pristine CNTs, *f*-CNTs show an obvious smaller length–diameter ratio and are homo-disperse without serious entanglement, shown in Figure 1b. Improved dispersion of *f*-CNTs was thus shown to be conducive to the preparation of CNTs-reinforced matrix composites.

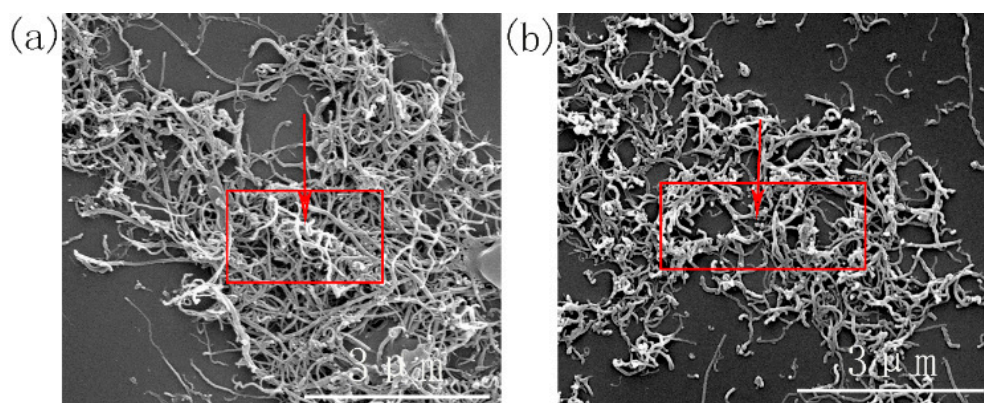


Figure 1. The morphology of (a) pristine CNTs and (b) *f*-CNTs.

To further characterize the structures, the obtained *f*-CNTs were characterized by XPS and TGA, as shown in Figure 2. It is obvious in Figure 2a, that the C1s spectrum of acidulated CNTs can be quantitatively differentiated into four different carbon species (O=C–O, C=O, C–O, and C–C/C=C). Moreover, the intensity of the C–O peak at 286.0 eV is marked, indicating successful preparation of *f*-CNTs [31]. Figure 2b presents TGA and DTG curves of pristine CNTs and *f*-CNTs. Pristine CNTs show excellent thermal stability and a slight decomposition appears above 600 °C. In comparison to that of pristine CNTs, *f*-CNTs show slight decomposition beginning at about 250 °C and an obvious weight loss appearing at about 310 °C, which can be assigned to the decomposition of oxygen functional groups, including hydroxyl, carboxyl groups, and others. DTG curves shown in Figure 2b, in which peaks appears at about 250 °C and 600 °C all correspond to changes of TGA curves. Moreover, on evaluating the decomposition processes of *f*-CNTs, the total weight loss shown in Figure 2b can also be assigned to the introduction of oxygen functional groups, that is, *f*-CNTs possess about 12 wt% oxygen functional groups. Thus, assisted by XPS tests and thermal stability measurements, the structures of *f*-CNTs were confirmed and the content of oxygen functional groups was also evaluated. Scheme 1 shows the preparation diagram of *f*-CNTs.

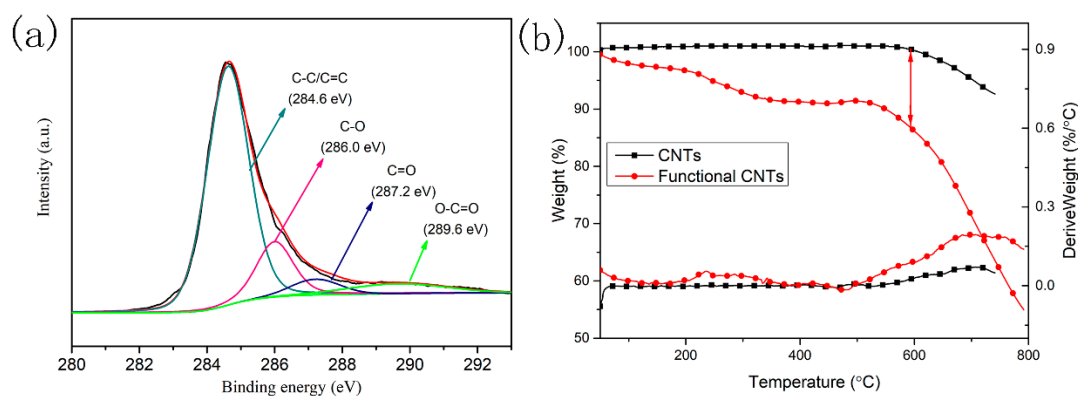
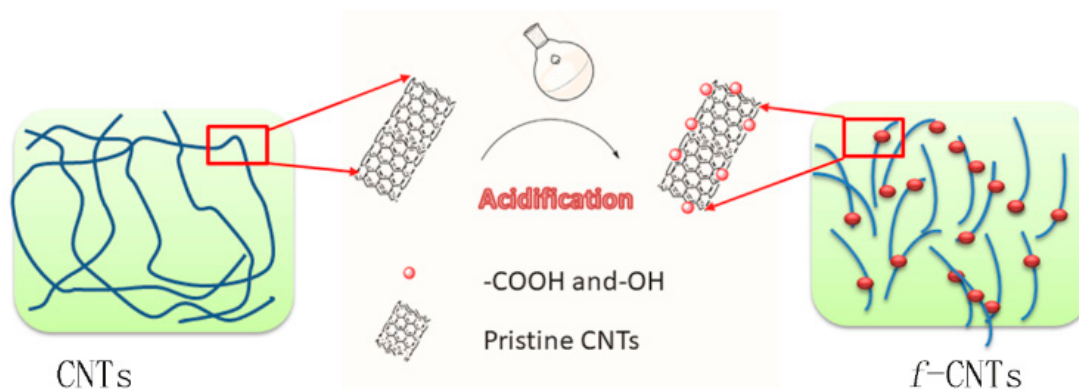


Figure 2. (a) XPS spectra and (b) TGA curves of *f*-CNTs.



Scheme 1. Preparation of functional CNTs (*f*-CNTs).

3.2. Curing Behaviors of *h*-BN/*f*-CNTs Reinforced Matrix Blends

According to our previous work, CE/AG80 blends filled with *h*-BN (40 wt%) were prepared and their curing behaviors characterized by DSC [28]. In this work, one of the aims was to reveal the influence of *f*-CNTs on the curing processes of the matrix resin. Thus, *h*-BN reinforced matrix resins with various contents of *f*-CNTs were investigated as shown in Figure 3. The shapes of DSC curves are usually used to reveal the curing processes, including the initial curing temperatures, peak curing temperatures, and post-curing temperatures. The detailed thermal properties of AG80/CE/*h*-BN with various contents of *f*-CNTs are collated in Table 2. In Figure 3, it is obvious that the main exothermic peak at about 250 °C can be assigned to copolymerization of CE and AG80 [32]. The approximate exothermic peaks indicate that the various contents of *f*-CNTs do not show any obvious influence on the curing behaviors of the resin matrix. Moreover, the fact that exothermic peaks appear at 320 °C, assigned to post-curing processes, also indicates that the main polymerizations of matrix resin are not affected by *f*-CNTs. However, compared with that of the resin matrix without *f*-CNTs, the initial curing temperatures of the resin matrix with *f*-CNTs shift to low temperature range, indicating that the *f*-CNTs may trigger copolymerization of CE and AG80. To summarize, the introduction of *f*-CNTs cannot significantly promote the main polymerization of resin matrix, but may trigger the reaction and initiate initial curing behavior in the low temperature range.

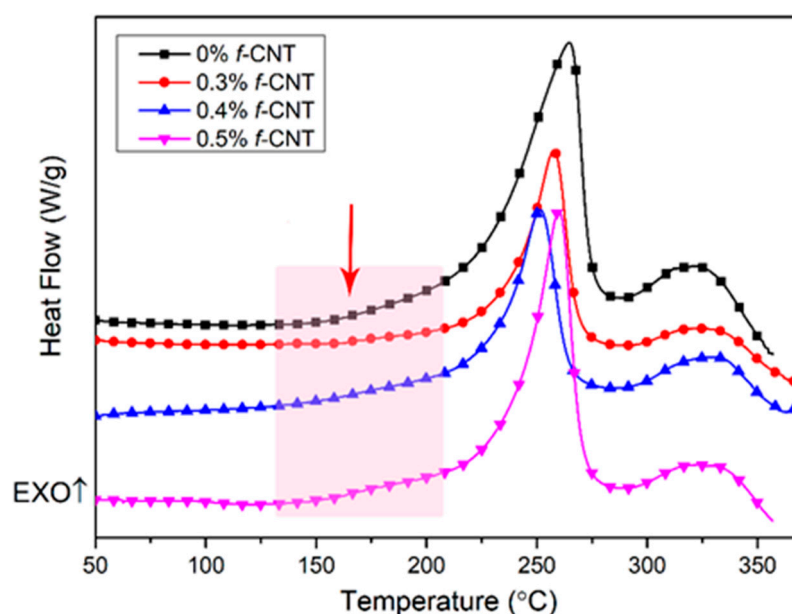


Figure 3. Curing behavior of *h*-BN/*f*-CNTs reinforced matrix blends.

Table 2. Thermal properties of AG80/CE/h-BN with various contents of *f*-CNTs.

Samples	$T_{initial}$ (°C)	T_{peak} (°C)	T_{post} (°C)
0% <i>f</i> -CNTs	170	258	325
0.3% <i>f</i> -CNTs	176	252	327
0.4% <i>f</i> -CNTs	162	243	329
0.5% <i>f</i> -CNTs	151	253	328

3.3. Thermal Conductivity of h-BN/*f*-CNT Reinforced Composites

The thermal conductivity (λ) values of h-BN/*f*-CNT reinforced resin matrix composites were investigated and the content of *f*-CNTs affecting the λ values of the resin matrix composites are shown in Figure 4. According to our previous work, the λ value of resin matrix with h-BN (40 wt%) is 0.54 W/mk [28]. Moreover, Agari's model was used to evaluate the effect of the h-BN fillers in the resin matrix and results indicated that it was difficult to create thermal conductive channels efficiently under conditions, according to low C_2 . In Figure 4a, on introduction of *f*-CNTs, the λ values of composites increase significantly, composites with 0.5 wt% *f*-CNTs show a λ value of 0.745 W/mk. Besides, on increasing the content of *f*-CNTs, λ values increase correspondingly, increasing from 0.648 W/mk (with 0.3 wt% *f*-CNTs) to 0.745 W/mk (with 0.5 wt% *f*-CNTs). The microphotographs of h-BN/*f*-CNT reinforced composites are also presented in Figure 4c–f. Simulative thermal conductivity channels according to percolation theory are shown in the microphotographs. This indicates that with the introduction of bits of *f*-CNTs, resin matrix composites with improved thermal conductivity can be obtained. The reason can be attributed to various factors: first, nanoscale CNTs show outstanding thermal conductivity themselves; second, *f*-CNTs contribute to repair defects inside the h-BN filled resin matrix composites, due to the microscale of h-BN and its discoid shape.

To confirm the effects of *f*-CNTs on forming thermal conductivity channels and networks of composites, Agari's semi-empirical model is employed [9]. Agari's model is based on the generalization of series and parallel conduction models in composites and correlates thermal conductivity with the ability of fillers to create particle conductive chains and is:

$$\log K_c = \varphi C_2 \log K_f + (1 - \varphi) \log C_1 K_p$$

where K_c , K_f , and K_p correspond to the thermal conductivity of composites, fillers, and polymer matrices, respectively. φ is the filler volume/weight fraction, C_1 and C_2 are obtained by fitting the experimental data. The logarithmic plot of thermal conductivity with respect to filler content is presented in Figure 4b, and the two parameters C_1 and C_2 were calculated to be 0.872 and 0.336. The value of C_1 suggests that the introduction of *f*-CNTs affects the curing processes of the resin matrix, similar to that of h-BN and decreases the crosslinking degree of the matrices. The value of C_2 indicates the ability to form conductivity channels and networks. In comparison with that of the resin matrix with pristine h-BN ($C_2 = 0.1593$), the C_2 (0.336) of composites with both h-BN and *f*-CNTs obviously increase. This visually shows that introduction of *f*-CNTs has improved the ability to form thermal conductivity channels and networks according to the percolation theory. Gu and his co-workers reported that combination of micrometer and nanometer BN fillers improved the thermal conductivity of resin matrix composites [2,5,6]. Thus, for CE/AG80/h-BN composites, the main heat transfer is dependent on conductivity channels forming with h-BN, which is defective due to the difficulty to form and stack-up discoid h-BN. After adding *f*-CNTs, conductivity channels and networks are easier to form and defective channels and networks will be repaired by *f*-CNTs, resulting in an improved thermal conductivity value [21,26].

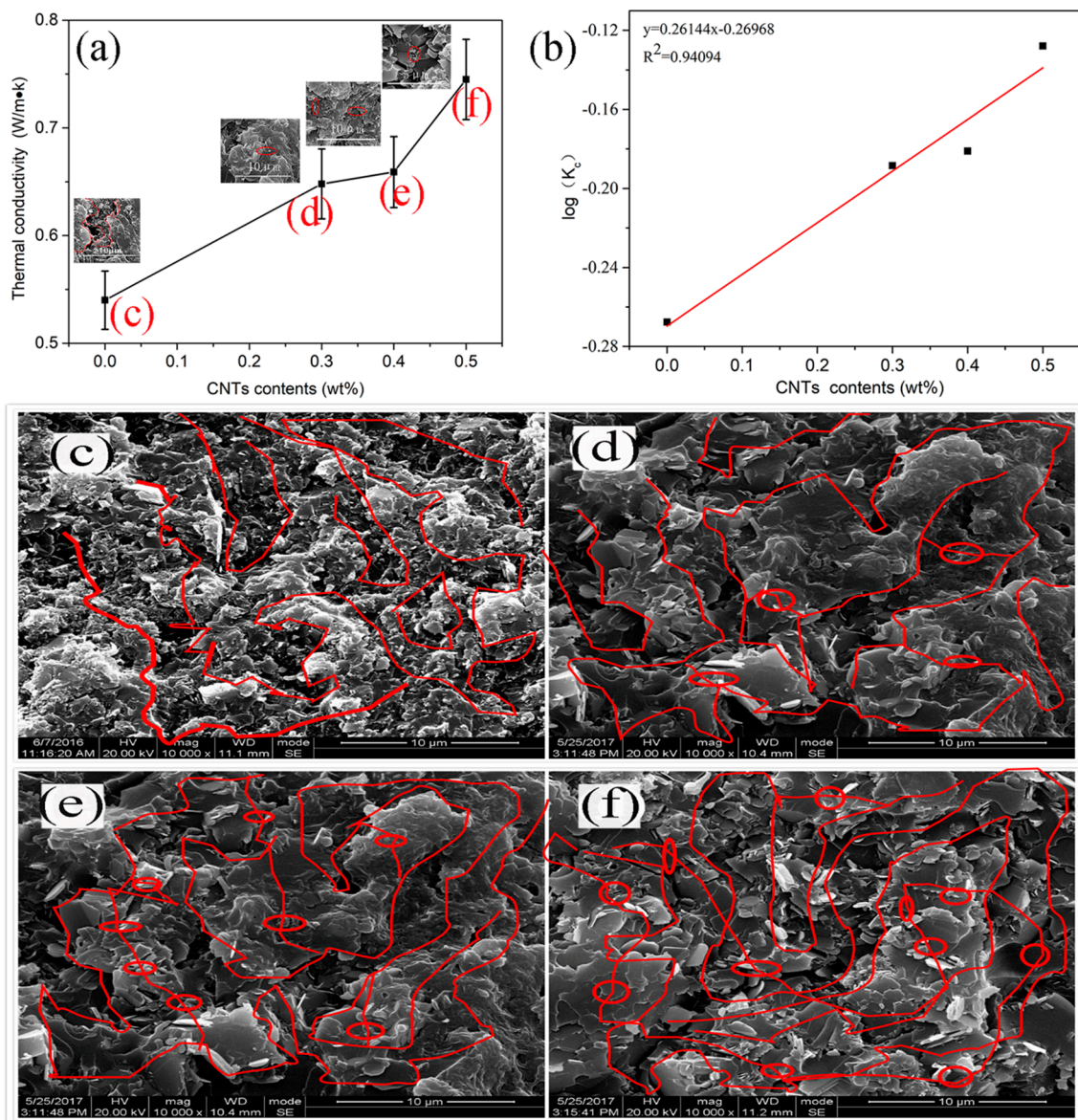
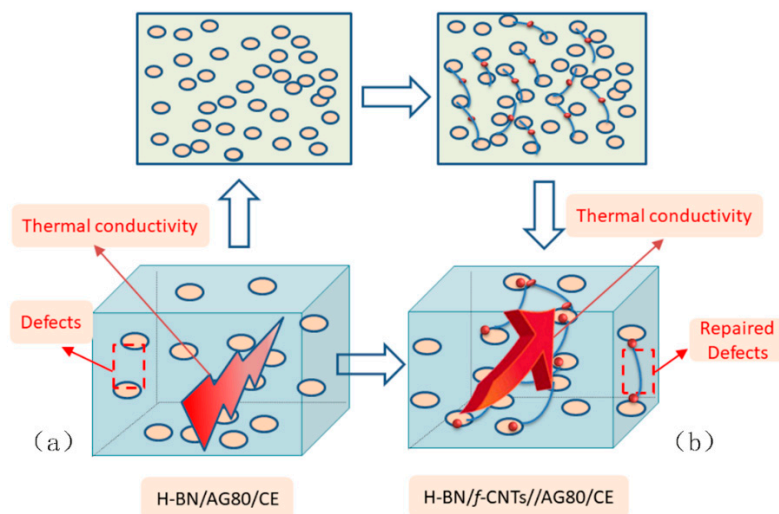


Figure 4. The thermal conductivity of h-BN/*f*-CNTs reinforced composites: (a) the content of *f*-CNTs affecting on λ value of resin matrix composites; (b) logarithmic plot of λ values with respect to the content of *f*-CNTs (Agari's model); (c) microphotographs of h-BN reinforced composites; (d) h-BN/*f*-CNTs reinforced composites with 0.3 wt% *f*-CNTs; (e) with 0.4 wt% *f*-CNTs and (f) with 0.5 wt% *f*-CNTs.

Scheme 2 shows the possible route of forming improved conductivity channels and networks, with both h-BN and *f*-CNTs. As shown in Scheme 2a, primary conductivity channels are constructed with discoid h-BN. However, due to the microscale of h-BN, channels exist with obvious defects, that limit the improvement of the thermal conductivity. With the introduction of *f*-CNTs, the defects of the conductivity channels are repaired via interconnect effects of *f*-CNTs and h-BN shown in Scheme 2b. With contact of *f*-CNTs and h-BN, the channels and networks become perfect and thermal conductivity will increase correspondingly.



Scheme 2. Possible forming mode of improved thermal conductivity channels and networks: (a) forming of thermal conductivity channels with h-BN and (b) forming of thermal conductivity channels with both h-BN and *f*-CNTs.

3.4. Fracture Surface of h-BN/*f*-CNT Reinforced Composites

Figure 5 shows the fracture surface of resin matrix composites with both h-BN and *f*-CNTs. Figure 5a, b show pristine h-BN and resin matrix. Obviously, discoid h-BN with uniform size of ~100 nm diameter, stacks, and aggregates are in view [28]. The pristine resin matrix shows a smooth fracture surface, indicating the typical brittle fracture. With addition of h-BN, the smooth fracture surface disappears as in Figure 5c. It has been reported that mutual contact and overlap of h-BN in the matrix exists and primary conductivity channels and networks are formed [2]. With addition of *f*-CNTs, the fracture surfaces of resin matrix with both h-BN and *f*-CNTs are different (Figure 5d–f), in which CNTs can be observed (labeled with red circles) and are dispersed uniformly. Combining the results of the thermal conductivity values of composites with *f*-CNTs shown in Figure 4a, the introduction of *f*-CNTs has contributed to forming perfect conductivity channels. Thus, the uniform dispersion of *f*-CNTs may just fix the defects resulting from random distribution of h-BN. Moreover, on increasing the content of *f*-CNTs, the CNTs in view increase as shown in Figure 5d–f.

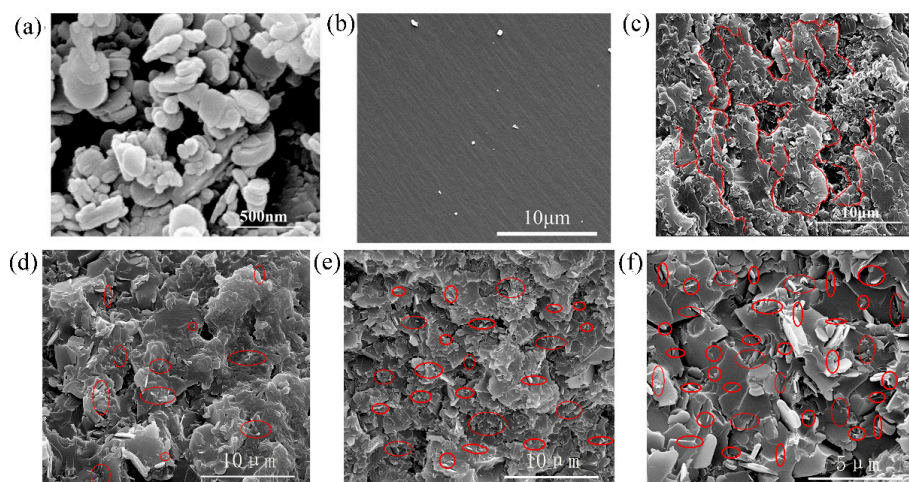


Figure 5. Fractural images of h-BN/*f*-CNT reinforced composites: (a) pristine h-BN; (b) pristine resin matrix; (c) resin matrix with h-BN (40 wt%); (d) resin matrix with both h-BN (40 wt%) and *f*-CNTs (0.3 wt%); (e) resin matrix with both h-BN (40 wt%) and *f*-CNTs (0.4 wt%), and (f) resin matrix with both h-BN (40 wt%) and *f*-CNTs (0.5 wt%).

3.5. Mechanical Properties of h-BN/f-CNTs Reinforced Composites

The mechanical properties of h-BN/f-CNTs composites determine their applications in the fields of functional-structural materials. Figure 6 shows the flexural strength and flexural modulus of the resin matrix with various contents of *f*-CNTs. It can be seen that the flexural strength of the pristine resin matrix composites shows an excellent value (72 MPa). With introduction of h-BN (40 wt%), the strength of the composites shows a slight decrease to 65 MPa. The strength decrease of the composites can be due to micro-scale h-BN in the resin matrix that may hinder polymerization and decrease the crosslinking degree. With addition of *f*-CNTs, the flexural strength of the composites increases correspondingly on increasing the content of *f*-CNTs. The obvious increase of flexural strength can be assigned to the reinforcement of nanoscale particles in the resin matrix. As is well known, the mechanical properties of resin matrix composites are mainly determined by the polymerization degree of the resin matrix and the dispersion of fillers in the resin matrix. Thus, in this work, the improvement of mechanical properties can be ascribed to the following factors: (1) the polymerization degree of composites may be improved with introduction of *f*-CNTs. As mentioned above, DSC results show that the initial polymerization temperatures of the resin matrix shift to low temperature ranges with the addition of *f*-CNTs, indicating the promotion effects of *f*-CNTs on the copolymerization of the matrix. (2) uniform dispersion of h-BN and *f*-CNTs may be also contributing to the perfect microstructures of composites, which will result in improved mechanical properties. By combining the fracture surface of the composites shown in Figure 5, it can be observed that h-BN and *f*-CNTs are uniformly dispersed in the matrix, which may synergistically improve the combination properties of the matrix composites. Figure 6 also shows the flexural modulus of composites with various contents of *f*-CNTs. Modulus values of composites increase correspondingly on increasing the content of *f*-CNTs. A similar variation trend of flexural strength and modulus also indicates that the introduction of *f*-CNTs significantly improves the mechanical properties of composites.

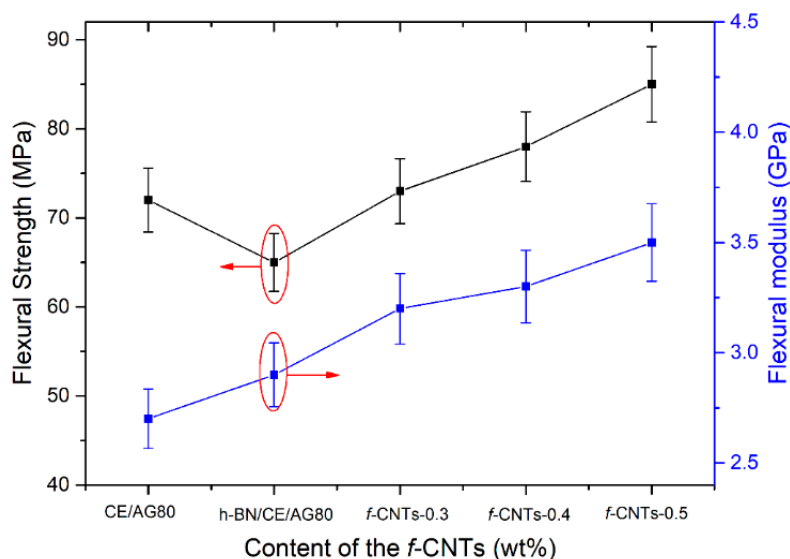


Figure 6. Flexural strength and modulus of resin matrix composites with both h-BN and *f*-CNTs.

3.6. Thermal-Mechanical Properties of h-BN/f-CNTs Reinforced Composites

DMA measurements were applied to measure tan delta and the storage modulus. In Figure 7, the storage modulus and glass transition temperatures of h-BN/CE/AG80 composites with various *f*-CNTs contents are presented. Moreover, the values of the storage modulus at 50 °C are listed in Table 2. As reported, the dynamic properties represent the value of the energy dissipated in the strain process and the value of energy in the composite stored as elastic energy. On addition of fillers, geometrical characteristics, weight fraction, dispersion with resin matrix and load transfer from

filler to matrix may influence the modulus to a great extent. In Figure 7a, the storage modulus of composites with 0.3 wt% and 0.4 wt% *f*-CNTs are higher than that of AG80/CE composites with just h-BN. The increase of storage modulus can be ascribed to the improvement of polymerization degree and the perfect microstructures of the composites. The composites with 0.5 wt% *f*-CNTs shows the lowest modulus, it may be attributed to aggregation of h-BN and *f*-CNTs, which introduces defects into the matrix. To summarize, all of the composites with both *f*-CNTs and h-BN show outstanding storage modulus and composites with moderate content of *f*-CNTs show higher modulus than that of composites with just h-BN, which also indicates synergetic enhancement of *f*-CNTs and h-BN on the thermal-mechanical properties of the composites.

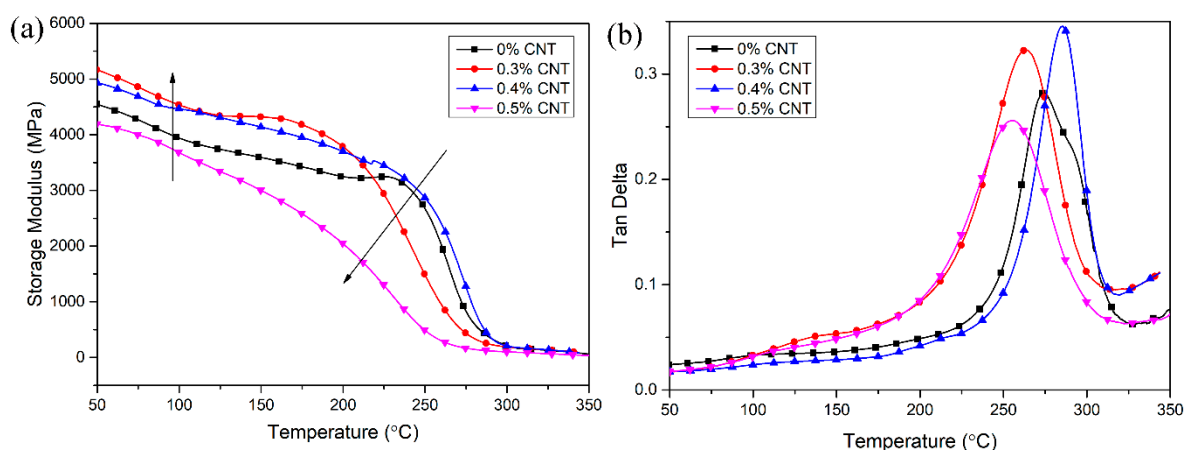


Figure 7. DMA curves of h-BN/*f*-CNTs reinforced composites: (a) storage modulus and (b) tan delta.

Figure 7b presented plots of $\tan \delta$ for composites with various contents of *f*-CNTs. It was reported that $\tan \delta$ is usually used to reveal glass transition temperatures (T_g) of resin matrix composites. Detailed data of the glass transition temperatures are summarized in Table 3. It is obvious that T_g s show similar values (~ 260 °C) for composites with various contents of *f*-CNTs, indicating that the T_g s of resin matrix composites have not been affected significantly by fillers. In comparison, composites with 0.4 wt% *f*-CNTs show the highest T_g value (285.2 °C), indicating that addition of *f*-CNTs can improve the thermal property of composites to some extent.

Table 3. Thermal properties of h-BN/*f*-CNTs reinforced composites.

Sample	DMA			TGA	
	Storage Modulus (GPa)	T_g (°C)	$T_{5\%}$ (°C)	$T_{10\%}$ (°C)	Char Yield (%)
h-BN-40%	4.5	274.7	346.8	357.7	53.4
h-BN-40%- <i>f</i> -CNTs-0.3%	5.1	262.9	378.5	392.6	56.4
h-BN-40%- <i>f</i> -CNTs-0.4%	4.9	285.2	387.7	398.8	51.9
h-BN-40%- <i>f</i> -CNTs-0.5%	4.2	255.5	383.1	395.7	57.9

Thermal stabilities of resin matrix composites with various contents of *f*-CNTs were characterized by TGA as shown in Figure 8 and the detailed data are collated in Table 3, in which the temperatures at weight loss of 5% ($T_{5\%}$), 10% ($T_{10\%}$), and char yield at 600 °C are displayed. According to Figure 8, it is obvious that composites with both *f*-CNTs and h-BN show higher decomposition temperatures than that of composites with just h-BN. Moreover, on increasing the content of *f*-CNTs, the decomposition of composites is almost constant. It can be explained by the fact that the addition of *f*-CNTs has improved the polymerization degree of the resin matrix but the content of *f*-CNTs shows no obvious effects on the copolymerization degrees. Additionally, the DTG curves of composites are also presented in Figure 8. The curve shapes are similar, indicating a similar decomposition mechanism. As reported,

it can be concluded that introduction of *f*-CNTs will increase the copolymerization degree to some extent but not change the decomposition process of AG80/CE composites.

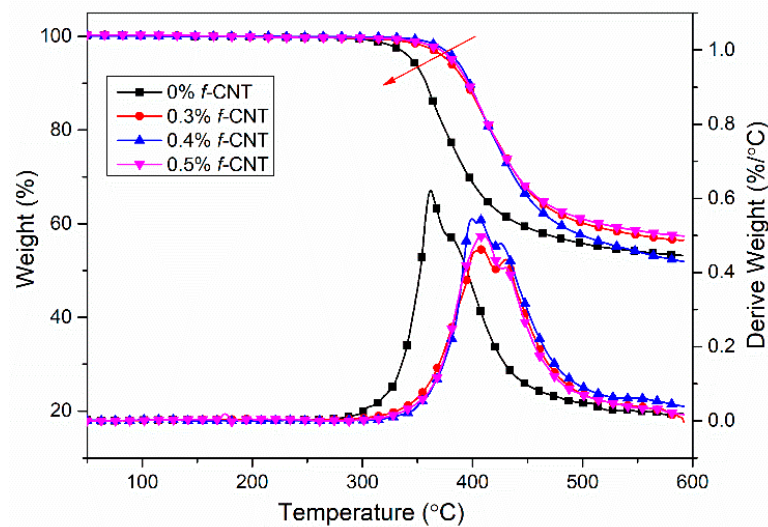


Figure 8. Thermal stability of h-BN/*f*-CNT reinforced composites.

4. Conclusions

Synergetic enhancement of *f*-CNTs and h-BN on the combination properties of AG80/CE matrix composites was confirmed by investigation of thermal conductivity values, flexural strength and modulus, thermal-mechanical properties, and thermal stability. Results indicated that on introduction of *f*-CNTs, λ values increase by 38% from 0.54 W/mk to 0.745 W/mk for composites with 0.5 wt% *f*-CNTs. Agari's model also shows that *f*-CNTs are conducive to forming conductivity channels and networks. Flexural strength (65–85 MPa) and modulus (2.7–3.5 GPa) also increase on introduction of *f*-CNTs, indicating enhancement of nanoparticles on mechanical properties. Combining storage modulus (4.2–5.1 GPa) and T_g s (255–285 °C) properties, the enhancement of *f*-CNTs on thermal-mechanical properties of composites is significant, especially for composites with 0.4 wt% *f*-CNTs having been introduced. In summary, various investigations on combination properties of resin matrix composites with both h-BN and *f*-CNTs were implemented and synergetic enhancement of h-BN and *f*-CNTs was confirmed. Moreover, AG80/CE resin matrix composites with both h-BN and *f*-CNTs possess good thermal conductivity and thermal-mechanical properties, and can be used as candidates for applications for functional and structural materials. On considering both thermal conductivity and thermal mechanical properties, the introduction of 0.4 wt% *f*-CNTs may be a good method to fabricate satisfactory composites.

Author Contributions: Conceptualization, M.X.; Methodology, Y.L.; Validation, X.L.; Investigation and Data Curation, D.R.; Writing—Original Draft Preparation, M.X.; Writing—Review and Editing, M.X.; Visualization, M.X.; Funding Acquisition, M.X.

Funding: This research was funded by National Natural Science Foundation of China, grant number 51803020 and The APC was funded by 51803020.

Acknowledgments: The authors gratefully thank the financial support from National Natural Science Foundation of China (Project No. 51803020)

Conflicts of Interest: The authors declare no conflict of interest.

References

1. Song, N.; Yang, J.; Ding, P.; Tang, S.; Shi, L. Effect of polymer modifier chain length on thermal conductive property of polyamide 6/graphene nanocomposites. *Compos. Part A Appl. Sci. Manuf.* **2015**, *73*, 232–241. [[CrossRef](#)]

2. Gu, J.W.; Meng, X.D.; Tang, Y.S.; Li, Y.; Zhuang, Q.; Kong, J. Hexagonal boron nitride/polymethyl-vinyl siloxane rubber dielectric thermally conductive composites with ideal thermal stabilities. *Compos. Part A Appl. Sci. Manuf.* **2017**, *92*, 27–32. [[CrossRef](#)]
3. Gu, J.; Yang, X.; Lv, Z.; Li, N.; Liang, C.; Zhang, Q. Functionalized graphite nanoplatelets/epoxy resin nanocomposites with high thermal conductivity. *Int. J. Heat Mass Transf.* **2016**, *92*, 15–22. [[CrossRef](#)]
4. Xingyi, H.; Chunyi, Z.; Pingkai, J.; Dmitri, G.; Yoshio, B.; Toshikatsu, T. Polyhedral Oligosilsesquioxane-Modified Boron Nitride Nanotube Based Epoxy Nanocomposites: An Ideal Dielectric Material with High Thermal Conductivity. *Adv. Funct. Mater.* **2013**, *23*, 1824–1831.
5. Gu, J.W.; Lv, Z.Y.; Wu, Y.L.; Guo, Y.Q.; Tian, L.D.; Qiu, H.; Li, W.Z.; Zhang, Q.Y. Dielectric thermally conductive boron nitride/polyimide composites with outstanding thermal stabilities via in-situ polymerization-electrospinning-hot press method. *Compos. Part A Appl. Sci. Manuf.* **2017**, *94*, 209–216. [[CrossRef](#)]
6. Gu, J.W.; Guo, Y.Q.; Yang, X.T.; Liang, C.B.; Geng, W.C.; Tang, L.; Li, N.; Zhang, Q.Y. Synergistic improvement of thermal conductivities of polyphenylene sulfide composites filled with boron nitride hybrid fillers. *Compos. Part A Appl. Sci. Manuf.* **2017**, *95*, 267–273. [[CrossRef](#)]
7. Li, C.M.; Tan, J.J.; Gu, J.W.; Xue, Y.; Qiao, L.; Zhang, Q.Y. Facile synthesis of imidazole microcapsules via thiol-click chemistry and their application as thermally latent curing agent for epoxy resins. *Compos. Sci. Technol.* **2017**, *142*, 198–206. [[CrossRef](#)]
8. Gu, J.W.; Xu, S.; Zhuang, Q.; Tang, Y.S.; Kong, J. Hyperbranched Polyborosilazane and Boron Nitride Modified Cyanate Ester Composite with Low Dielectric Loss and Desirable Thermal Conductivity. *IEEE Trans. Dielectr. Electr. Insul.* **2017**, *24*, 784–790. [[CrossRef](#)]
9. Agari, Y.; Ueda, A.; Nagai, S. Thermal conductivity of a polymer composite. *J. Appl. Polym. Sci.* **1993**, *49*, 1625–1634. [[CrossRef](#)]
10. Gu, J.; Liang, C.; Zhao, X.; Gan, B.; Qiu, H.; Guo, Y.; Yang, X.; Zhang, Q.; Wang, D.-Y. Highly thermally conductive flame-retardant epoxy nanocomposites with reduced ignitability and excellent electrical conductivities. *Compos. Sci. Technol.* **2017**, *139*, 83–89. [[CrossRef](#)]
11. Shen, X.; Wang, Z.; Wu, Y.; Liu, X.; He, Y.-B.; Kim, J.-K. Multilayer Graphene Enables Higher Efficiency in Improving Thermal Conductivities of Graphene/Epoxy Composites. *Nano Lett.* **2016**, *16*, 3585–3593. [[CrossRef](#)] [[PubMed](#)]
12. Gu, H.; Ma, C.; Gu, J.; Guo, J.; Yan, X.; Huang, J.; Zhang, Q.; Guo, Z. An overview of multifunctional epoxy nanocomposites. *J. Mater. Chem. C* **2016**, *4*, 5890–5906. [[CrossRef](#)]
13. Zha, J.W.; Dang, Z.M.; Li, W.K.; Zhu, Y.H.; Chen, G. Effect of micro-Si₃N₄-nano-Al₂O₃ co-filled particles on thermal conductivity, dielectric and mechanical properties of silicone rubber composites. *IEEE Trans. Dielectr. Electr. Insul.* **2014**, *21*, 1989–1996. [[CrossRef](#)]
14. Zhou, Y.; Bai, Y.; Yu, K.; Kang, Y.; Wang, H. Excellent thermal conductivity and dielectric properties of polyimide composites filled with silica coated self-passivated aluminum fibers and nanoparticles. *Appl. Phys. Lett.* **2013**, *102*, 252903. [[CrossRef](#)]
15. Huang, X.; Iizuka, T.; Jiang, P.; Ohki, Y.; Tanaka, T. Role of Interface on the Thermal Conductivity of Highly Filled Dielectric Epoxy/AlN Composites. *J. Phys. Chem. C* **2012**, *116*, 13629–13639. [[CrossRef](#)]
16. Gu, J.-W.; Zhang, Q.; Zhang, J.; Wang, W. Studies on the Preparation of Polystyrene Thermal Conductivity Composites. *Polym.-Plast. Technol. Eng.* **2010**, *49*, 1385–1389. [[CrossRef](#)]
17. Kusunose, T.; Yagi, T.; Firoz, S.H.; Sekino, T. Fabrication of epoxy/silicon nitride nanowire composites and evaluation of their thermal conductivity. *J. Mater. Chem. A* **2013**, *1*, 3440–3445. [[CrossRef](#)]
18. Jiang, Q.; Wang, X.; Zhu, Y.; Hui, D.; Qiu, Y. Mechanical, electrical and thermal properties of aligned carbon nanotube/polyimide composites. *Compos. Part B-Eng.* **2014**, *56*, 408–412. [[CrossRef](#)]
19. Xu, L.; Chen, G.; Wang, W.; Li, L.; Fang, X. A facile assembly of polyimide/graphene core-shell structured nanocomposites with both high electrical and thermal conductivities. *Compos. Part A Appl. Sci. Manuf.* **2016**, *84*, 472–481. [[CrossRef](#)]
20. Choi, S.; Kim, J. Thermal conductivity of epoxy composites with a binary-particle system of aluminum oxide and aluminum nitride fillers. *Compos. Part B-Eng.* **2013**, *51*, 140–147. [[CrossRef](#)]
21. Seran, C.; Hyungu, I.; Jooheon, K. The thermal conductivity of embedded nano-aluminum nitride-doped multi-walled carbon nanotubes in epoxy composites containing micro-aluminum nitride particles. *Nanotechnology* **2012**, *23*, 065303.

22. Zhang, P.; Li, Q.; Xuan, Y. Thermal contact resistance of epoxy composites incorporated with nano-copper particles and the multi-walled carbon nanotubes. *Compos. Part A Appl. Sci. Manuf.* **2014**, *57*, 1–7. [[CrossRef](#)]
23. Wang, R.; Zhuo, D.; Weng, Z.; Wu, L.; Cheng, X.; Zhou, Y.; Wang, J.; Xuan, B. A novel nanosilica/graphene oxide hybrid and its flame retarding epoxy resin with simultaneously improved mechanical, thermal conductivity, and dielectric properties. *J. Mater. Chem. A* **2015**, *3*, 9826–9836. [[CrossRef](#)]
24. Huang, T.; Zeng, X.; Yao, Y.; Sun, R.; Meng, F.; Xu, J.; Wong, C. Boron nitride@graphene oxide hybrids for epoxy composites with enhanced thermal conductivity. *RSC Adv.* **2016**, *6*, 35847–35854. [[CrossRef](#)]
25. Zhou, T.; Wang, X.; Cheng, P.; Wang, T.; Xiong, D.; Wang, X. Improving the thermal conductivity of epoxy resin by the addition of a mixture of graphite nanoplatelets and silicon carbide microparticles. *Express Polym. Lett.* **2013**, *7*, 585–594. [[CrossRef](#)]
26. Yu, A.; Ramesh, P.; Sun, X.; Bekyarova, E.; Itkis, M.E.; Haddon, R.C. Enhanced Thermal Conductivity in a Hybrid Graphite Nanoplatelet—Carbon Nanotube Filler for Epoxy Composites. *Adv. Mater.* **2008**, *20*, 4740–4744. [[CrossRef](#)]
27. Ngo, I.-L.; Prabhakar Vattikuti, S.V.; Byon, C. Effects of thermal contact resistance on the thermal conductivity of core-shell nanoparticle polymer composites. *Int. J. Heat Mass Transf.* **2016**, *102*, 713–722. [[CrossRef](#)]
28. Lei, Y.; Han, Z.; Ren, D.; Pan, H.; Xu, M.; Liu, X. Design of h-BN-Filled Cyanate/Epoxy Thermal Conductive Composite with Stable Dielectric Properties. *Macromol. Res.* **2018**, *26*, 602–608. [[CrossRef](#)]
29. Samantray, P.K.; Karthikeyan, P.; Reddy, K.S. Estimating effective thermal conductivity of two-phase materials. *Int. J. Heat Mass Transf.* **2006**, *49*, 4209–4219. [[CrossRef](#)]
30. Xu, M.; Hu, J.; Zou, X.; Liu, M.; Dong, S.; Zou, Y.; Liu, X. Mechanical and thermal enhancements of benzoxazine-based GF composite laminated by in situ reaction with carboxyl functionalized CNTs. *J. Appl. Polym. Sci.* **2013**, *129*, 2629–2637. [[CrossRef](#)]
31. Wei, R.; Wang, J.; Wang, Z.; Tong, L.; Liu, X. Magnetite-Bridged Carbon Nanotubes/Graphene Sheets Three-Dimensional Network with Excellent Microwave Absorption. *J. Electron. Mater.* **2017**, *46*, 2097–2105. [[CrossRef](#)]
32. Lei, Y.; Xu, M.; Jiang, M.; Huang, Y.; Liu, X. Curing behaviors of cyanate ester/epoxy copolymers and their dielectric properties. *High Perform. Polym.* **2017**, *29*, 1175–1184. [[CrossRef](#)]



© 2018 by the authors. Licensee MDPI, Basel, Switzerland. This article is an open access article distributed under the terms and conditions of the Creative Commons Attribution (CC BY) license (<http://creativecommons.org/licenses/by/4.0/>).